*Send Orders for Reprints to reprints@benthamscience.net*

*Progress in Nanoscience and Nanotechnology,* xxxx, *x,* xxxxxx

**RESEARCH ARTICLE**

# Sustainable Fabrication of Onion-Peel Biogenic Silica Nanoparticles for Multimodal Characterization and *In Vitro* Bioactivity Profiling

Sphoorty Hungund[1], Raghunandan Deshpande[2], Arun K. Shettar[3] and Gurushantappa Kadakol[4,*]

*[1]Department of Applied Science and Technology, BLDE (Deemed to be University), Vijayapura 586103, Karnataka, India; [2]H.K.E.S.'s Matoshree Taradevi Rampure Institute of Pharmaceutical Sciences, Sedam Road, Kalaburagi 585105, Karnataka, India; [3]Multidisciplinary Research Unit, Karnataka Medical College and Research Institute, Hubballi 580022, Karnataka, India; [4]Genetics Laboratory, School of Applied Science and Technology, BLDE (Deemed to be University), Vijayapura 586103, Karnataka, India*

**ARTICLE HISTORY**

Received: January 27, 2026
Revised: March 20, 2026
Accepted: April 07, 2026

DOI:
*10.2174/0131173640478030260514115522*

**Abstract:** ***Introduction*:** This study aims to develop a sustainable method for synthesizing Biogenic Silica Nanoparticles (bSNPs) from onion peel waste and evaluate their physicochemical properties and *in vitro* bioactivity.

***Methods*:** Biogenic Silica Nanoparticles (bSNPs) were prepared via an optimized acid–base sol–gel method and characterized by SEM, EDX, AFM, FTIR, and XRD. Antioxidant activity (DPPH assay), anti-inflammatory activity (protein denaturation), and DNA interaction (agarose gel) were assessed *in vitro*.

***Results*:** Biogenic Silica Nanoparticles (bSNPs) exhibited nanoscale dimensions (~120–125 nm) with spheroidal morphology and rough surface characteristics. FTIR and XRD confirmed amorphous silica. Dose-dependent antioxidant and anti-inflammatory activity, as well as DNA binding, were observed.

***Discussions*:** Biogenic Silica Nanoparticles (bSNPs) were synthesized from onion peel biomass via a two-acid sol–gel process. Spectroscopic and crystallographic analyses confirmed the successful synthesis of homogeneous amorphous silica. bSNPs exhibited effective biomolecular interactions.

***Conclusion*:** Onion peel-derived bSNPs are durable, environmentally friendly nanomaterials with promising antioxidant, anti-inflammatory, and DNA-binding potential for biomedical applications.

**Keywords:** Biogenic silica nanoparticles, onion peel Agro-waste, sol–gel synthesis, antioxidant activity, anti-inflammatory activity, DNA binding.

## 1. INTRODUCTION

Nanotechnology involves the manipulation of atoms and molecules to develop materials with unique and functional properties [1, 2]. The distinctive characteristics of nanoparticles have enabled significant advancements in biomedical science, particularly in drug delivery, diagnostics, and therapeutic applications [3]. In recent years, there has been growing interest in green synthesis approaches for the production of metal nanoparticles, in which plant-derived biomolecules serve as natural reducing and stabilizing agents. These methods highlight the critical role of plant extracts in the controlled synthesis and surface modification of nanoparticles [4]. Currently, there is increasing emphasis on the development of sustainable nanomaterials through eco-friendly synthesis strategies that utilize renewable resources such as agricultural waste. Such approaches not only reduce environmental impact but also enhance the biocompatibility of the resulting materials [5, 6]. Nanotechnology is one of the fastest-growing scientific fields, with expanding applications in electronics, aerospace, defense, biological sciences, and dental research [7]. At the nanoscale, materials exhibit unique physicochemical properties compared to their bulk counterparts, enabling them to be transformed into highly functional materials. Nanoparticles (NPs), derived from metals, semiconductors, magnetic materials, or composites, have significantly impacted biomedical science due to their enhanced biological interactions. These properties make them suitable for applications such as drug delivery, gene transfer, imaging diagnostics, hyperthermia, wound healing, tissue engineering, and biolabeling [8, 9]. The agricultural sector generates large quantities of waste annually, including sugarcane bagasse, corn cobs, rice husk, and wheat straw, which are often improperly managed or burned, leading to environmental pollution and degradation [10].

*Address correspondence to this author at the Genetics Laboratory, School of Applied Science and Technology, BLDE (Deemed to be University), Vijayapura 586103, Karnataka, India; E-mail: gs.kadakol@bldedu.ac.in

  

Agricultural waste generated at various stages, including cultivation, harvesting, processing, and production, contains a wealth of valuable organic and inorganic components that remain largely underutilized [11]. Improper waste management leads to greenhouse gas emissions, soil and water contamination, and potential health risks for humans and animals [12]. Therefore, sustainable strategies for waste reduction and reutilization are essential for environmental protection and future resource sustainability [13]. The conversion of agricultural waste into value-added products directly supports circular and green economy principles. Functional nanomaterials can be sustainably synthesized from by-products such as coconut husk, fruit peels and seeds, rice bran, maize cobs, wheat husk, and palm oil waste. These materials demonstrate significant potential for applications in industrial and biomedical fields [14-16].

Bioactive compounds and carrier systems enabling targeted and sustained release are increasingly important in modern drug delivery strategies. Conventional biocides such as azoles, carbamates, pyrethroids, and copper-based compounds are often incorporated into polymeric matrices [17]. However, these polymer-based systems may be costly, unstable, and environmentally non-persistent[18]. In contrast, silica-based materials, particularly mesoporous silica and silica nano capsules, have garnered considerable attention as drug delivery vehicles due to their high surface area, tunable pore structure, and excellent thermal and chemical stability. Despite these advantages, conventional methods for synthesizing silicon dioxide nanoparticles are often expensive and environmentally unfriendly.[19] Previous studies on silica nanoparticles derived from agricultural waste such as rice husk, maize cob, and sugarcane bagasse have reported particle sizes ranging from 80 to 150 nm, along with DPPH radical scavenging activity between 30% and 70% at concentrations of 50–200 μg/mL. However, despite the generation of approximately 47 million tonnes of onion waste annually worldwide, limited research has explored the synthesis of silica nanoparticles from onion peels [20].

Onion peels are rich in flavonols and other phytochemicals, indicating their potential as a valuable precursor for nanoparticle synthesis. This gap highlights the need for systematic evaluation of the size, purity, and bioactivity of silica nanoparticles derived from onion waste. Biogenic silica nanoparticles produced from natural sources represent a green and sustainable alternative with promising applications in topical and biomedical drug delivery systems [21].

Conventional methods for synthesizing silica nanoparticles, including thermal decomposition, microwave-assisted synthesis, laser-induced deposition, hydrogen plasma growth, and hydrothermal techniques, are often energy-intensive and require hazardous chemicals or sophisticated instrumentation. These limitations have driven the development of greener synthesis approaches, particularly those utilizing Agro-waste as a precursor [22]. Onion (*Allium cepa*) is the second most widely cultivated horticultural crop globally, producing approximately 47 million tonnes annually. The non-edible onion peel is typically discarded during processing, despite being rich in bioactive compounds with antioxidant, antibacterial, and anti-inflammatory properties [23]. Valorization of onion peel waste aligns with global sustainability goals and offers potential applications in the food, cosmetic, and pharmaceutical sectors. While the edible portion of the onion has been extensively studied, the peel remains a relatively underexploited by-product. Therefore, comprehensive chemical and biological investigations are essential to fully exploit its potential as a sustainable precursor for nanoparticle synthesis [24, 25]. In this study, Biogenic Silica Nanoparticles (bSNPs) were synthesized from onion peel waste using a modified acid–base sol–gel method. Unlike previous studies that have primarily focused on rice husk and sugarcane bagasse, this work explores onion peel as an alternative, sustainable source. The synthesized nanoparticles were extensively characterized using SEM, AFM, FTIR, XRD, and EDS techniques. Furthermore, *in vitro* assays were conducted to evaluate antioxidant, anti-inflammatory, and DNA-binding activities. This study uniquely integrates sustainable material synthesis with comprehensive physicochemical and biological characterization.

## 2. MATERIALS AND METHODS

### 2.1. Materials

The schematic representation of the experimental workflow, including precursor preparation, synthesis, purification, and characterization steps, is shown in Fig. (**1**). All chemicals and reagents were of analytical grade and obtained from standard commercial suppliers (HiMedia, India). The reagents were used from institutional stock; therefore, individual Catalog numbers were not recorded at the time of experimentation. However, all reagents are traceable through institutional procurement records.

Onion peels with minimal moisture were obtained from a grocery vendor in Gulbarga. All solutions were prepared using distilled water, and the chemical procedures involved only high-quality hydrochloric acid and sodium hydroxide [26].

### 2.2. Preparation of Onion Peel Aqueous Extract (OPE)

The outer dried layers of onion peel were obtained from a local trader in Gulbarga. These peels, chosen for their low moisture content and uniform size, were thoroughly cleaned with distilled water to remove any dust or dirt. After cleaning, the peels were air-dried at room temperature (about 25°C) until they attained a steady weight. To create the extract, 5 grams of dried peels were added to a 1000-mL flask with distilled water and boiled in a water bath at 100°C for 30 minutes. After cooling, the mixture was filtered to create a clear Onion Peel Extract (OPE) that was stored in sterile amber bottles at 4°C until needed [27, 28].

### 2.3. Sol–Gel Process for Nanoparticle Synthesis

Silica nanoparticles were created using a modified sol-gel process, with onion peels serving as a natural source of silica. The dried peels were initially exposed to acid and heat treatments in order to eliminate metallic impurities and residual organic materials. The biomass was macerated and treated with 10% hydrochloric acid (HCl) followed by 30% sulfuric acid ($H_2SO_4$) for demineralization and breakdown of the lignocellulosic structure. The acid-treated peels were

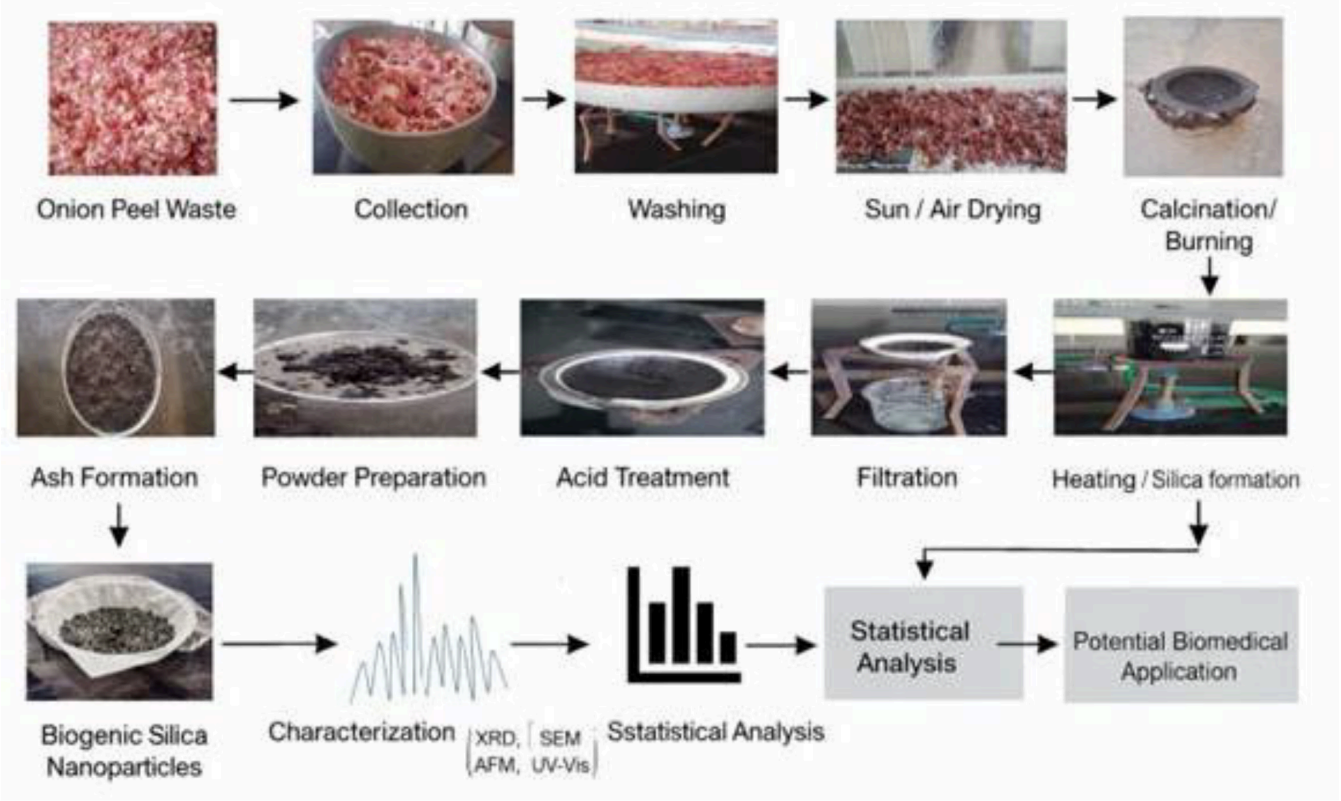


**Fig. (1).** Schematic representation of the experimental workflow for the synthesis and characterization of silica nanoparticles, including preparation of precursor solution, synthesis process, purification, and characterization using XRD, SEM, and zeta potential analysis. *(A higher resolution / colour version of this figure is available in the electronic copy of the article).*

calcined in a muffle furnace at 600°C for 4 hours to produce silica-rich ash through full carbonization and hydrocarbon volatilization. The calcined powder was refluxed with 10% HCl and 30% $H_2SO_4$ at 100 °C for 2 hours in a 3-neck round-bottom flask with a condenser and heating mantle. This promoted the leaching of leftover metal ions and organic residues. The resultant slurry was filtered and rinsed many times with distilled water until the filtrate achieved neutral pH (~7), removing unreacted acids and soluble contaminants before proceeding with the sol-gel procedure [29, 30].

### 2.4 Preparation of Sodium Silicate Solution

To extract silica from pre-treated onion peel, 3.5 M sodium hydroxide (NaOH) was used, a common approach for dissolving biogenic silica into sodium silicate. The plant material was treated and heated, then combined with NaOH and heated at 100°C for 5 hours. This procedure helped to completely dissolve the silica. During heating, the silica in the material reacted with NaOH, yielding the following reaction:

$$SiO_2 + 2NaOH \rightarrow Na_2SiO_3 + H_2O \quad (1)$$

The mixture was filtered to remove insoluble residues. The filtrate was washed several times with boiling distilled water to remove residual impurities. The clean sodium silicate solution was then left to cool down to room temperature before moving on to the sol–gel process [31].

### 2.5. Synthesis of Silica Nanoparticles

The final product, obtained after sol–gel transition of the sodium silicate solution, was a fine white colloidal silica powder corresponding to nanosized silica. To preserve its structure and prevent moisture absorption, the prepared silica powder was stored in a desiccator until further characterization and application. The obtained nanoparticles were washed and dried at 60 °C for 12 h [31].

### 2.6. Characterization of Synthesized Nanoparticles

#### *2.6.1. UV–Vis Spectroscopy*

A Shimadzu UV-1800 spectrophotometer was used to record the nanoparticles' UV-Vis spectra. The optical characteristics of biogenic silica nanoparticles were assessed by collecting absorption spectra in the 200–800 nm range and calibrating the instrument using ultrapure water as a blank [31].

#### *2.6.2. FTIR Studies*

A Shimadzu IR Spirit-X Fourier Transform Infrared (FTIR) spectrometer was used to examine functional groups and chemical structure. In order to identify siloxane (Si–O–Si) networks, spectra were recorded at room temperature in the mid-infrared region (4000–400 $cm^{-1}$) and baseline correction was applied using the instrument software [32].

### *2.6.3. SEM Studies*

Surface morphology of the prepared nanoparticles was investigated by using a ZEISS scanning electron microscope. SEM operated at an accelerating voltage of 15 kV and a probe current of approximately 50 pA. Prior to recording, focus and contrast were adjusted as needed, and high magnification micrographs were acquired to assess the nanoparticle's size, shape, and surface characteristics [33].

### *2.6.4. XRD Studies*

X-ray diffraction (XRD) was used to characterize the crystalline and amorphous phases of silica nanoparticles at 40 kV and 30 mA using Cu Kα radiation (λ = 1.5406 Å). In order to identify silica polymorphs and evaluate peak broadening for structural analysis, patterns were captured over 2θ = 10–80° [34].

### *2.6.5. AFM Studies*

Bruker Dimension Icon AFM in tapping mode was used to examine nanoscale surface topography and particle distribution. Images were taken at a 1 Hz line rate over a 5 μm × 5 μm scan area to record height and phase data [35].

### *2.6.6. Zeta Potential Studies*

Surface charge and colloidal stability were measured with a HORIBA zeta potential analyser at 25 °C and 90° scattering angle. To prevent multiple scattering, samples were diluted in deionized water, and measurements were made three times [36].

### *2.6.7. Transmission Electron Microscopy (TEM)*

Characterization of the prepared biogenic nanosilica particles by TEM revealed their structure, size, and dispersion. Ethanol was used to suspend the nanoparticles, which were then drop-cast onto carbon-coated copper grids and allowed to dry at room temperature. Particle shape, size distribution, and aggregation were characterized by HRTEM imaging [37].

## 2.7. Biological Evaluation of Silica Nanoparticles

### *2.7.1. Antioxidant Study*

The DPPH assay was performed using standard laboratory reagents and methods described previously [37]. For the assay, 1.0 mL of freshly prepared DPPH solution (0.2 mM) was combined with 0.5 mL test sample solutions or a standard antioxidant (ascorbic acid; 50–250 μg/mL). To avoid the photodegradation of DPPH radical, reaction mixtures were incubated in the dark at room temperature for 30 minutes. The absorbance was then read at 517 nm using a Labman UV–Visible spectrophotometer after incubation.

The percentage of radical scavenging activity was calculated using the following equation:

$$\text{Antioxidant activity } (\%) = \frac{(A_c - A_s)}{A_c} \times 100 \qquad (2)$$

where A(c) represents the absorbance of the control, and A(s) represents the absorbance of the sample. The calculated values provide a quantitative assessment of the antioxidant potential of the synthesized Biogenic Silica Nanoparticles (bSNPs) [38].

### *2.7.2. Anti-Inflammatory Activity*

Phosphate-Buffered Saline (PBS) and Bovine Serum Albumin (BSA) were used for the assay. Protein denaturation involves modification of a protein's secondary and tertiary structures in response to external physicochemical stressors, such as high temperature, extreme pH, or increased ionic strength. [39] Preventing protein denaturation is an excellent *in vitro* technique for screening anti-inflammatory activity.

For the assay, 1.0 mL of Phosphate-Buffered Saline (PBS) was mixed with 50 μL of Bovine Serum Albumin (BSA) and different concentrations (50–250 μg/mL) of the test samples or the standard drug. The reaction mixtures sat at room temperature for 15 minutes, then were heated in a water bath at 70 °C for another 15 minutes to cause protein denaturation. Once cooled back to room temperature, their absorbance was measured at 660 nm using a Labman UV–Visible spectrophotometer.

We calculated how much the samples prevented protein denaturation using the following equation:

$$\text{Inhibition } (\%) = (A\_c - A\_t) / A\_c \times 100 \qquad (3)$$

Here, A(c) is the absorbance of the control sample, and A(t) is the absorbance of the treated sample. Aspirin was included as a reference drug for comparison [39, 40].

### *2.7.3. Binding Activity of DNA*

Agarose gel electrophoresis was performed using standard laboratory reagents. Agarose gel electrophoresis is a standard way to separate nucleic acids and study how molecules interact. For this test, 25 μL of genomic DNA was mixed with 25 μL of a silica nanoparticle suspension. To make this suspension, 100 mg of the nanoparticles were mixed with dimethyl sulfoxide (DMSO) and then diluted to 1 mL with distilled water. Ethidium bromide (EtBr) was added to help visualize the DNA.

The DNA samples mixed with nanoparticles were exposed to UV light for 1 hour, then left at room temperature for 3 hours. Untreated DNA acted as the control. Each experiment was done in triplicate. After incubation, the samples were run on agarose gels for electrophoresis to check how the DNA and nanoparticles interacted. If the DNA bands changed in brightness, position, or became smeared, it was taken as evidence that the DNA was binding to the silica. Example gel results are shown in the Results section [41].

## 2.8. Statistical Analysis

All experiments were performed in triplicate (n = 3) to ensure reproducibility, minimize experimental error, and provide statistically reliable mean values. Triplicate measurements are a standard practice in *in vitro* biological and analytical studies for preliminary validation of results. The obtained results are expressed as mean ± Standard Deviation (SD). The mean value was calculated using the following Equation:

$$x \doteq (1/n) \sum(i = 1 \text{ to } n)\ x\_i \quad (4)$$

where $x_i$ represents the individual measurement, and $n$ is the total number of observations.

The variability in the measurements was estimated using the Standard Deviation (SD), calculated according to the following Equation:

$$SD = \sqrt{\left[\frac{\sum(i=1 \text{ to } n)(x_i - \bar{x})^2}{(n-1)}\right]} \quad (5)$$

The Standard Error (SE), which represents the uncertainty associated with the mean value, was calculated using the following Equation:

$$SE = SD / \sqrt{n} \quad (6)$$

## 3. RESULTS

### 3.1. UV–Visible Spectroscopy (UV analysis)

Biogenic Silica Nanoparticles (bSNPs) were first formed and then checked using UV-Visible spectroscopy. To start, the baseline was set using the solvent, and a 0.05 mg/mL water-based sample was scanned from 200 to 800 nm with a 1 nm resolution (Fig. **2**). A strong absorption below 230 nm is linked to electronic transitions in the Si-O-Si network of silica. A faint shoulder between 280 and 320 nm likely comes from trace phytochemicals left from the plant-based synthesis. In the visible range (400–800 nm), there's no noticeable plasmonic absorption peak, which fits with the non-metallic, amorphous nature of these nanoparticles. The gradual baseline observed across the visible range is caused by light scattering and some clumping of nanoparticles in the suspension, not by contamination [42].

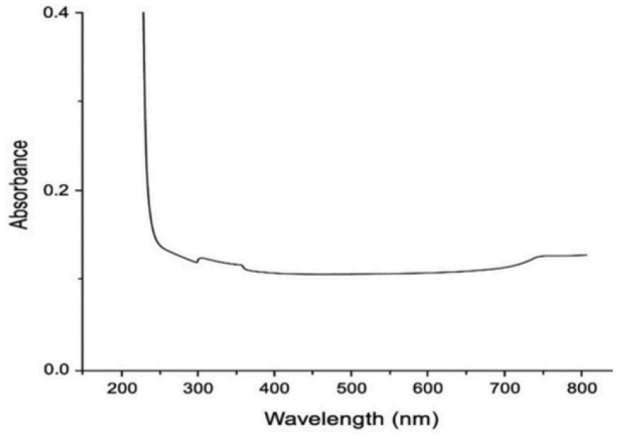


**Fig. (2).** UV–Visible absorption spectrum of biogenic silica nanoparticles showing the optical properties of the synthesized nanoparticles.

### 3.2. Fourier Transform Infrared Spectroscopy Analysis (FTIR)

FTIR spectroscopy was used to verify the chemical structure of the Biogenic Silica Nanoparticles (bSNPs) that were synthesized. The spectrum (Fig. **3**) displays a broad absorption band around 3300 $cm^{-1}$, which is due to O–H stretching vibrations from surface silanol (Si–OH) groups and water molecules adsorbed on the surface. A strong, sharp band at about 1088 $cm^{-1}$ matches the asymmetric stretching vibrations of the Si–O–Si network, a typical feature of amorphous silica. The band near 871 $cm^{-1}$ is linked to symmetric stretching of Si–O–Si bonds, while peaks at around 711 $cm^{-1}$ and 490 $cm^{-1}$ correspond to bending modes of the siloxane (Si–O–Si) structure. The lack of clear absorption bands for carbon-containing groups shows that organic residues were effectively removed during the calcination process. Altogether, the FTIR results confirm the successful formation of hydroxyl-rich, mostly amorphous $SiO_2$ nanoparticles, in agreement with earlier studies on biogenic silica.

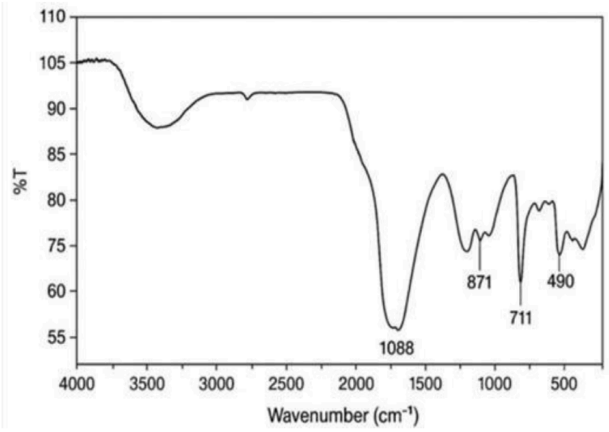


**Fig. (3).** FTIR spectrum of biogenic silica nanoparticles recorded in the range of 4000–400 $cm^{-1}$. The X-axis represents wavenumber ($cm^{-1}$) and the Y-axis represents percentage transmittance (%T).

### 3.3. Zeta Potential Analysis

Zeta potential analysis offered new perspectives in colloidal stability and surface charge characteristics of the synthesized nanoparticles (Figs. **4** and **5**).

Figures **4** and **5** show that when biogenic silica nanoparticles are dispersed at 1 mg/mL in purified water, they exhibit a nearly neutral zeta potential (−0.2 mV) at pH 5.0, which remains unchanged over a week of incubation. Since zeta potential values greater than ±30 mV indicate strong colloidal stability, the near-neutral surface charge seen here suggests there is limited electrostatic stabilization and a tendency for the particles to clump together, something typical for biogenic silica nanoparticles. This behaviour may be due to partial ionization of surface silanol (Si–OH) groups and the presence of leftover biomolecules from the onion peel used as the precursor. The nanoparticles also showed an average hydrodynamic diameter of about 150 nm in water, with slight differences likely due to aggregation or size variation, which matches previous reports of biosynthesized silica nanoparticles (Fig. **5**) [43].

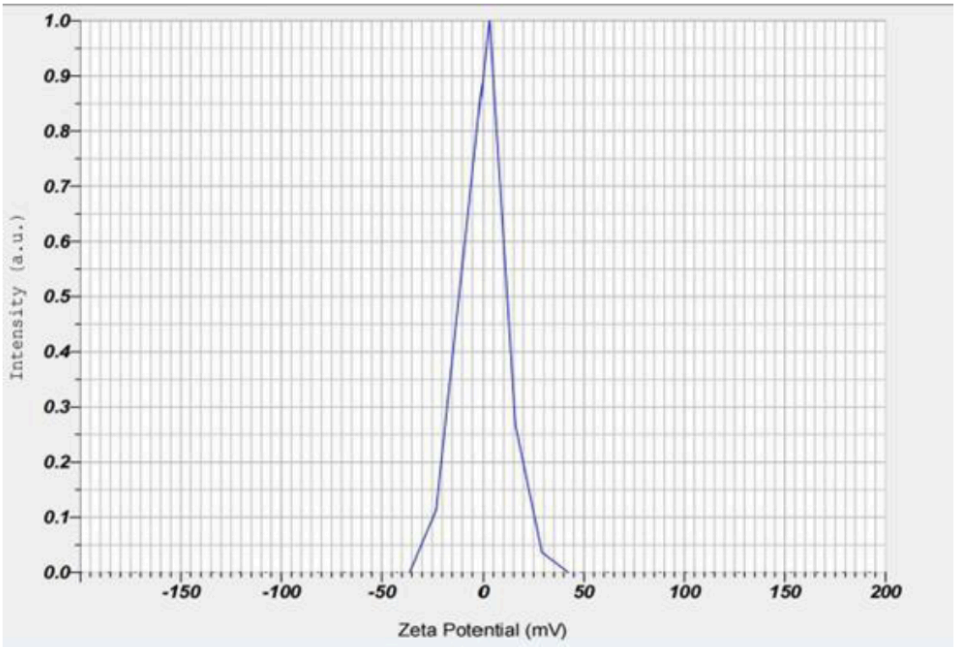


**Fig. (4).** Zeta potential distribution of synthesized silica nanoparticles, indicating limited electrostatic stabilization. *(A higher resolution / colour version of this figure is available in the electronic copy of the article).*

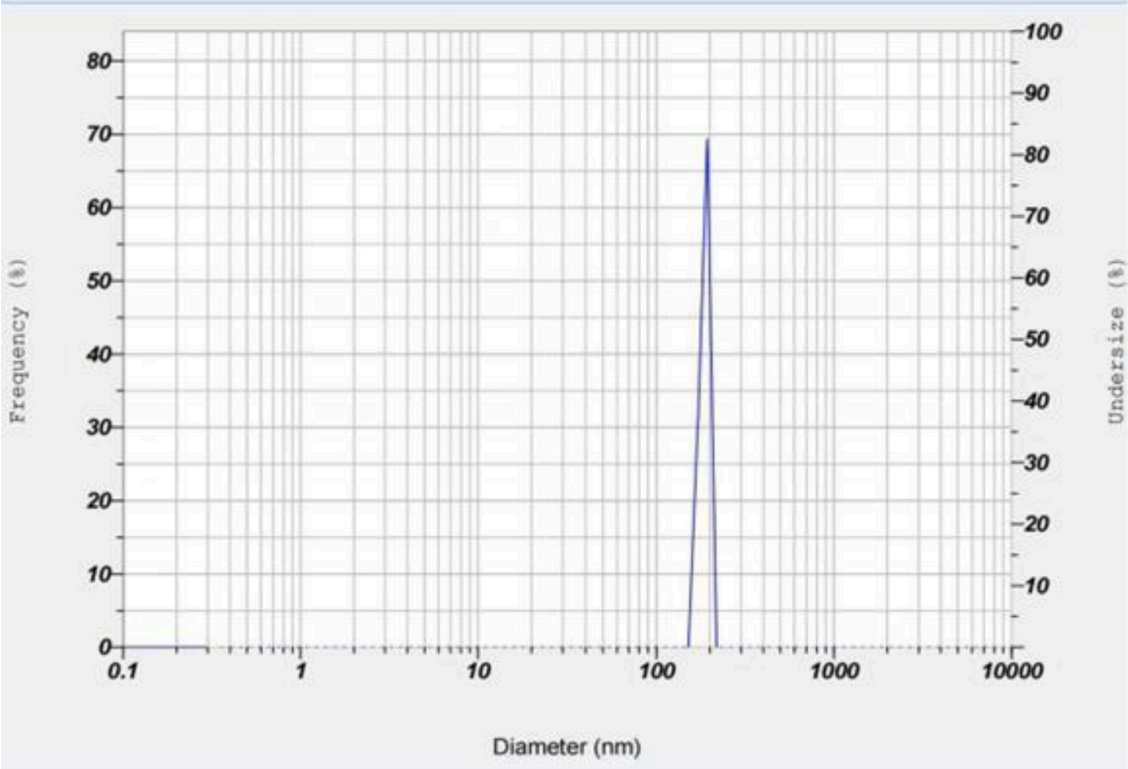


.

**Fig. (5).** Dynamic Light Scattering (DLS) analysis of silica nanoparticles shows an average hydrodynamic diameter of 150.3 nm, suggesting moderate particle aggregation in aqueous suspension. *(A higher resolution / colour version of this figure is available in the electronic copy of the article).*

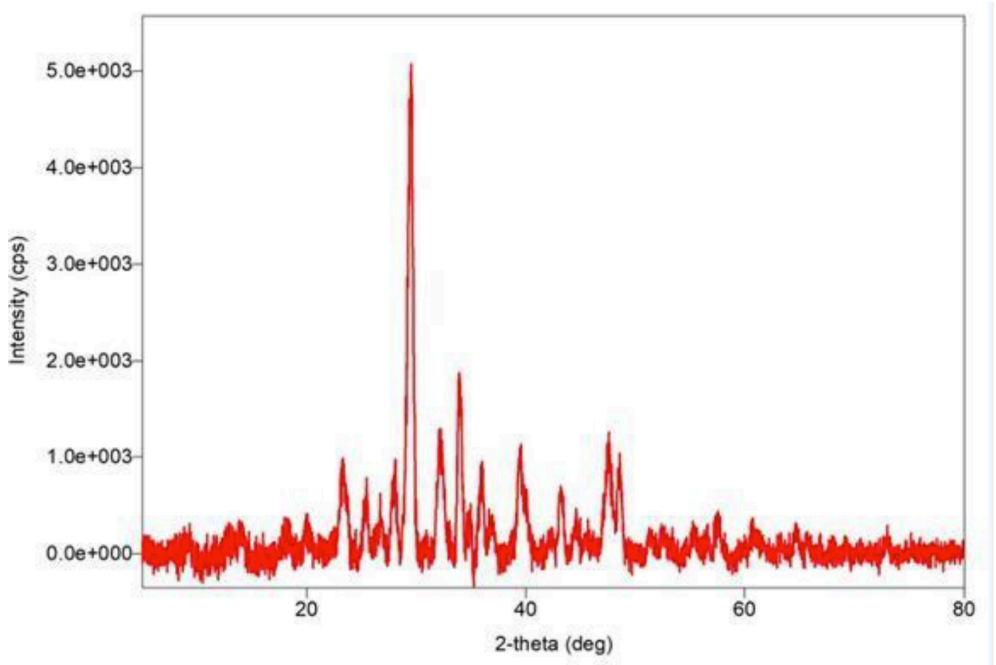


**Fig. (6).** X-Ray Diffraction (XRD) pattern of synthesized Biogenic Silica Nanoparticles (bSNPs). The diffraction profile shows several sharp reflections that may originate from trace crystalline mineral residues (e.g., potassium, calcium, or sodium salts) derived from the plant precursor. The absence of characteristic peaks corresponding to crystalline silica polymorphs such as quartz, cristobalite, or tridymite indicates that the silica matrix remains predominantly amorphous. *(A higher resolution / colour version of this figure is available in the electronic copy of the article).*

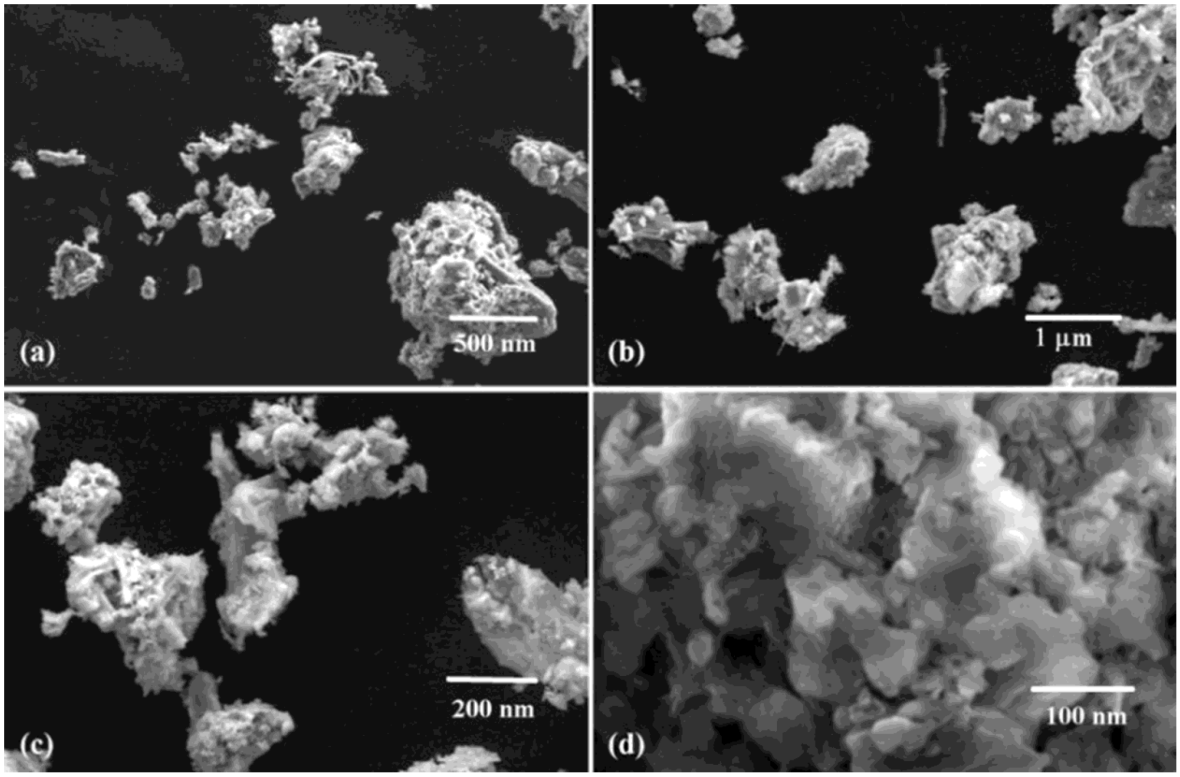


**Fig. (7).** SEM micrographs of synthesized Biogenic Silica Nanoparticles (bSNPs). (**a**) Aggregated nanoparticles (scale bar: 500 nm); (**b**) clustered structures at lower magnification (scale bar: 1 µm); (**c**) medium magnification showing irregular nanoparticle aggregates (scale bar: 200 nm); (**d**) high magnification revealing rough and porous surface morphology (scale bar: 100 nm). *(A higher resolution / colour version of this figure is available in the electronic copy of the article).*

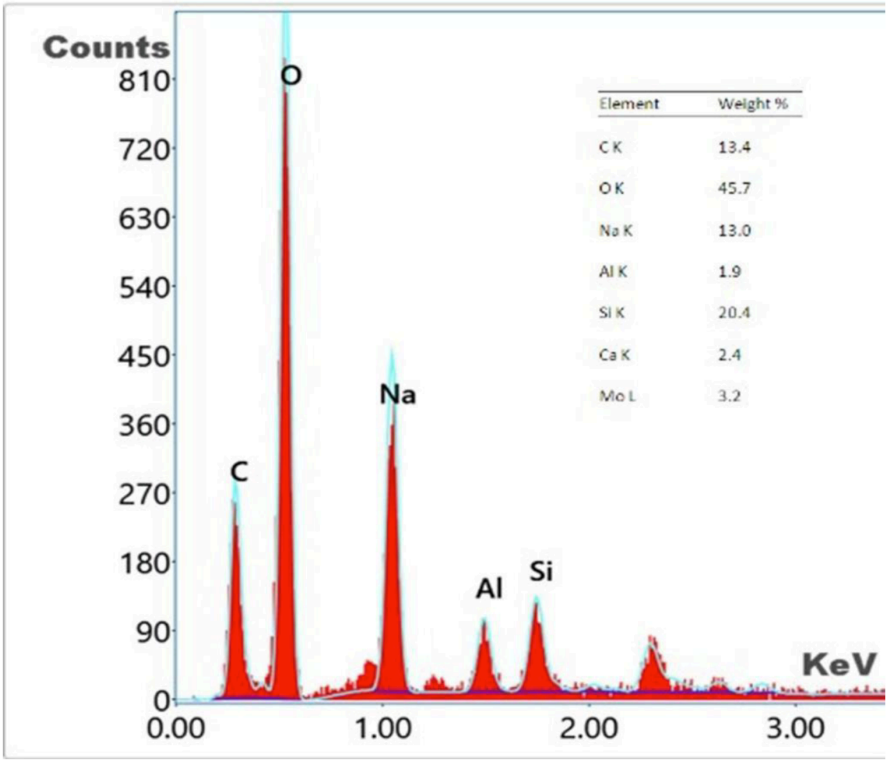


**Fig. (8).** EDX spectrum of synthesized Biogenic Silica Nanoparticles (bSNPs) showing elemental composition. The spectrum confirms the presence of silicon (Si) and oxygen (O) as the dominant elements, with minor traces of sodium (Na) and aluminium (Al). *(A higher resolution / colour version of this figure is available in the electronic copy of the article).*

### 3.4. X-Ray Diffraction Studies

XRD analysis was conducted to assess the structural phase (crystalline versus amorphous) of synthesized bSNPs (Fig. **6**).

X-ray diffraction (XRD) analysis was performed to characterize the structure of the synthesized Biogenic Silica Nanoparticles (bSNPs). The resulting diffraction pattern shows several sharp peaks scattered across the 2θ range, along with a faint diffuse background. These sharp peaks do not match the typical diffraction patterns of crystalline silica forms like quartz, cristobalite, or tridymite, as none of those characteristic peaks were found. Instead, the observed reflections likely come from tiny amounts of crystalline mineral residues left over from the plant material used in the synthesis. Plant biomass often contains inorganic elements like potassium, calcium, sodium, and magnesium, which can form crystalline salts or oxides during combustion or heating. Mineral-derived crystalline phases like these are often reported in plant-based or agricultural waste-derived silica materials. The presence of these minor crystalline reflections points to leftover inorganic components, not to the crystallization of the silica itself. As a result, the silica matrix produced in this study remains mostly amorphous, which agrees with previous reports on plant-derived biogenic silica nanoparticles [44].

### 3.5. Scanning Electron Microscopy (SEM)

Morphology of synthesized bSNPs was analysed through SEM (Fig. **7a**–**d**).

A diluted suspension of nanoparticles (0.1 mg/mL) was dropped onto a gold-coated silicon wafer and left to dry. Micrographs taken at various magnifications (Fig. **7a**–**d**) show that the nanoparticles tend to cluster together. At lower magnifications (Fig. **7a** and **b**), micron-sized clumps can be seen, formed when many smaller particles stick together during drying and deposition. This is common for silica nanoparticles due to their strong attraction to one another and the presence of surface silanol groups.

At higher magnifications (Fig. **7c** and **7d**), these larger clusters are shown to be made up of much smaller, nanoscale primary particles. The individual nanoparticles are irregular to almost spherical in shape and have rough, porous surfaces, features typical of biogenic silica. Judging by the scale bars, the primary particles are in the nanometer range, while the bigger structures are secondary aggregates. This rough, porous texture means the particles have a high surface area, confirming that the biogenic synthesis method successfully produced silica nanoparticles [45].

### 3.6. Elemental Analysis and Spectrum Processing (EDX)

Elemental makeup of synthesised bSNPs was confirmed by EDX analysis (Fig. **8**).

Energy Dispersive X-ray (EDX) analysis was used to check what elements are in the Biosynthesized Silica Nanoparticles (bSNPs). The EDX spectrum showed strong peaks for silicon (Si) and oxygen (O), confirming that the main component is silicon dioxide ($SiO_2$). These strong

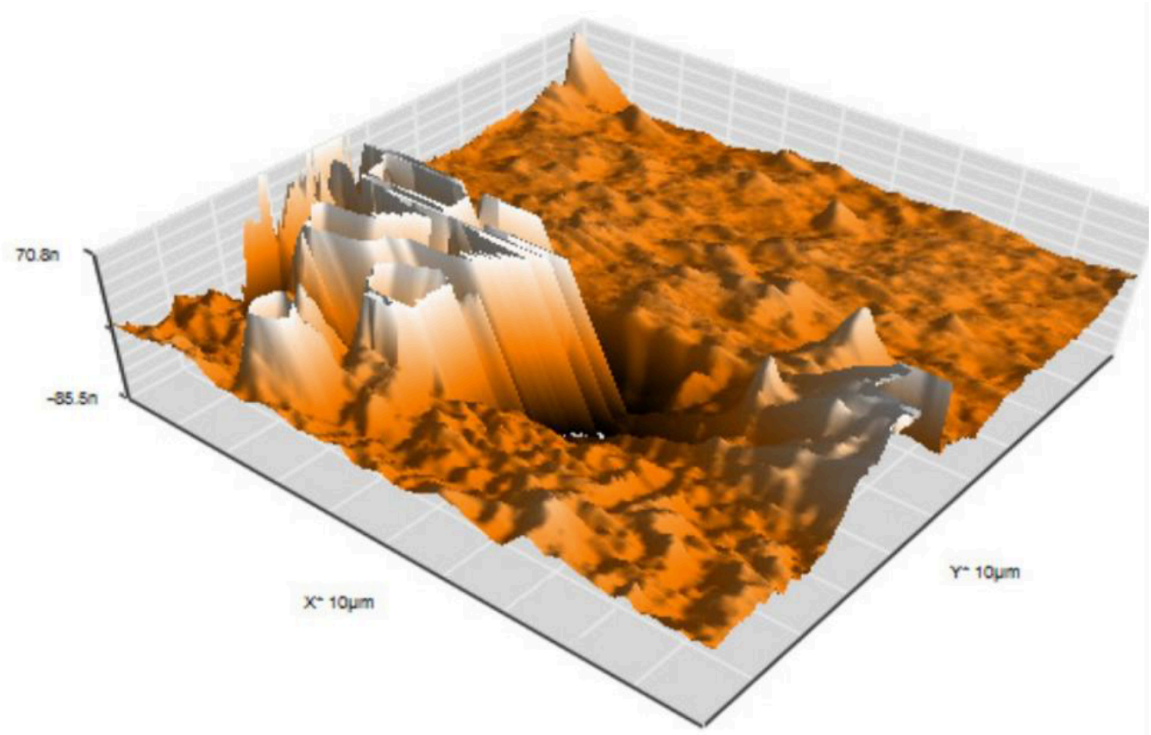


**Fig. (9).** AFM topographical images of synthesized Biogenic Silica Nanoparticles (bSNPs) showing three-dimensional surface morphology and surface roughness (scan area: 10 µm × 10 µm; height range: ~70 nm). *(A higher resolution / colour version of this figure is available in the electronic copy of the article).*

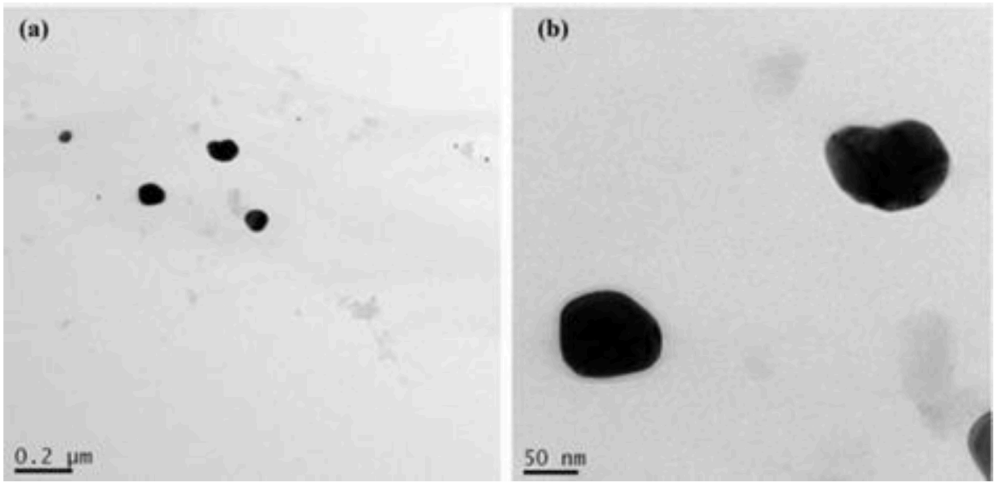


**Fig. (10).** TEM images of synthesized Biogenic Silica Nanoparticles (bSNPs): (**a**) low magnification showing particle distribution (scale bar: 200 nm); (**b**) high magnification showing near-spherical nanoparticles with nanoscale dimensions (scale bar: 50 nm). *(A higher resolution / colour version of this figure is available in the electronic copy of the article).*

signals mean the biogenic synthesis process successfully produced silica nanoparticles. A few smaller peaks for other elements may also appear, likely due to trace amounts of biomolecules from the biological extract or slight impurities from the sample substrate. Overall, the clear dominance of Si and O in the spectrum confirms that the nanoparticles are highly pure and were successfully synthesized.

### 3.7. Atomic Force Microscopy (AFM)

AFM imaging was used to analyse three-dimensional nanoscale surface morphology, including particle size, shape, and surface roughness (Fig. **9**).

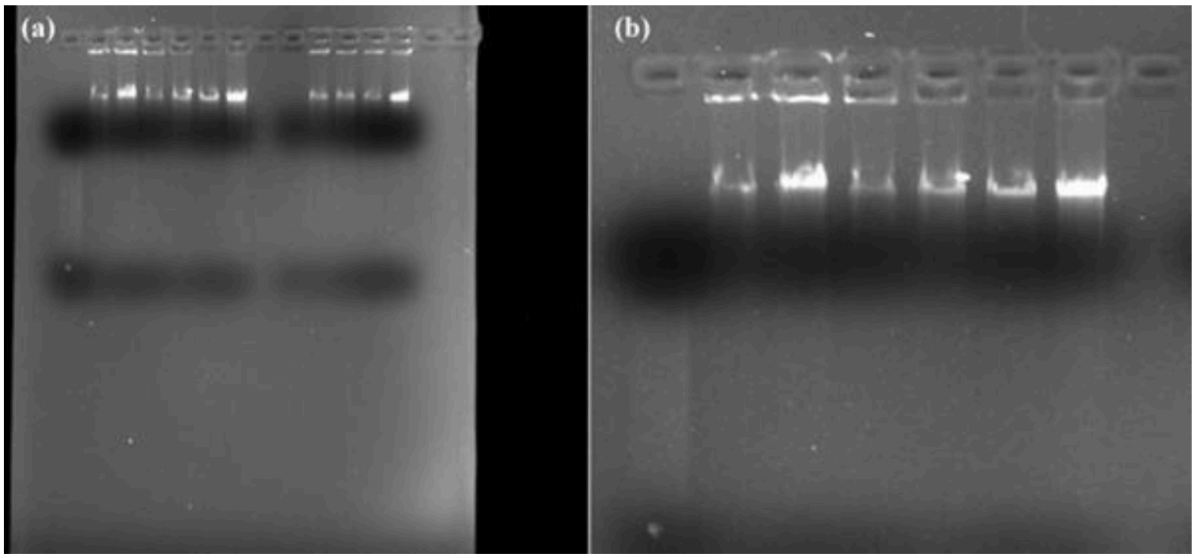


**Fig. (11).** Agarose gel electrophoresis demonstrating genomic DNA binding with Biogenic Silica Nanoparticles (bSNPs). (**a**) Free genomic DNA control showing normal migration. (**b**) Genomic DNA treated with increasing concentrations of bSNPs, exhibiting progressive retardation of DNA migration, indicating concentration-dependent DNA–bSNPs interaction. *(A higher resolution / colour version of this figure is available in the electronic copy of the article).*

Nanoparticles prepared from a 0.1 mg/mL aqueous suspension and deposited on a silicon substrate exhibited irregular morphology, with particle sizes ranging from 120 to 125 nm based on height profile analysis. High-resolution AFM images revealed uneven and rough surface textures, which are typical for biogenic silica systems. The tip–sample interaction parameters were optimized during imaging to ensure reliable topographical measurements.

The observed size of 120–125 nm corresponds to primary nanoparticles determined from localized height measurements within aggregated clusters. AFM images commonly show agglomerated structures due to strong interparticle interactions and surface silanol (Si–OH) groups, particularly in biogenic silica systems where clustering is frequently observed [46, 47].

### 3.8. Transmission Electron Microscopy

The analysis provided detailed structural information about the synthesized biogenic silica nanoparticles. At low magnification, the images showed loosely connected aggregates, indicating that the silica dispersions tend to clump together as they dry. At higher magnification, individual particles appeared nearly spherical to sub-spherical, with diameters ranging from 40 to 120 nm. The uniform internal electron density and the absence of crystalline lattice fringes confirm that the silica is amorphous, consistent with the XRD findings. The blurry particle edges and areas of higher density further support that the silica was successfully synthesized using the sol–gel method. In summary, Fig. (**10a**) shows a low-magnification image with loosely aggregated nanoparticles, while Fig. (**10b**) displays high-magnification images that reveal the spherical to sub-spherical shape of the particles. These observations confirm the nanoscale structure, amorphous nature, and aggregation behaviour of the onion-peel-derived bSNPs (Fig. **10a–b**) [48].

### 3.9. Interaction of Silica Nanoparticles with DNA Molecules

Agarose gel electrophoresis revealed significant binding interactions between bSNPs and genomic DNA (Fig. **11a–b**).

Fig. **11a-b** illustrates how genomic DNA interacts with Biogenic Silica Nanoparticles (bSNPs) during an agarose gel electrophoresis experiment. In the control lane, which contained no nanoparticles, the DNA migrated normally through the gel and formed a clear, sharp band, indicating that the DNA was intact and able to move freely. However, when silica nanoparticles were added, the DNA's movement through the gel decreased, and at higher nanoparticle concentrations, the DNA remained completely in the wells without migrating. This result indicates that the DNA strongly binds to the nanoparticles, forming large complexes that could not pass through the gel. This binding most likely occurs because positive ions act as bridges between the negatively charged phosphate groups in DNA and the silica surface, and through hydrogen bonding with the DNA bases. Such interactions are common for silica-based nanomaterials and play a crucial role in applications like gene delivery, biosensing, and DNA purification. The strong interaction between DNA and nanoparticles observed here suggests that these bSNPs have promising potential for use in biomedicine and biotechnology, particularly for carrying genetic material or other DNA-based applications [49, 50].

### 3.10. Antioxidant Activity

Antioxidant ability of the Biogenic Silica Nanoparticles (bSNPs) was tested using the DPPH radical scavenging assay [51] (Fig. **12a–d**). In the control sample, the average absorbance was 0.8421, confirming the presence of stable DPPH radicals. When bSNPs were added at increasing

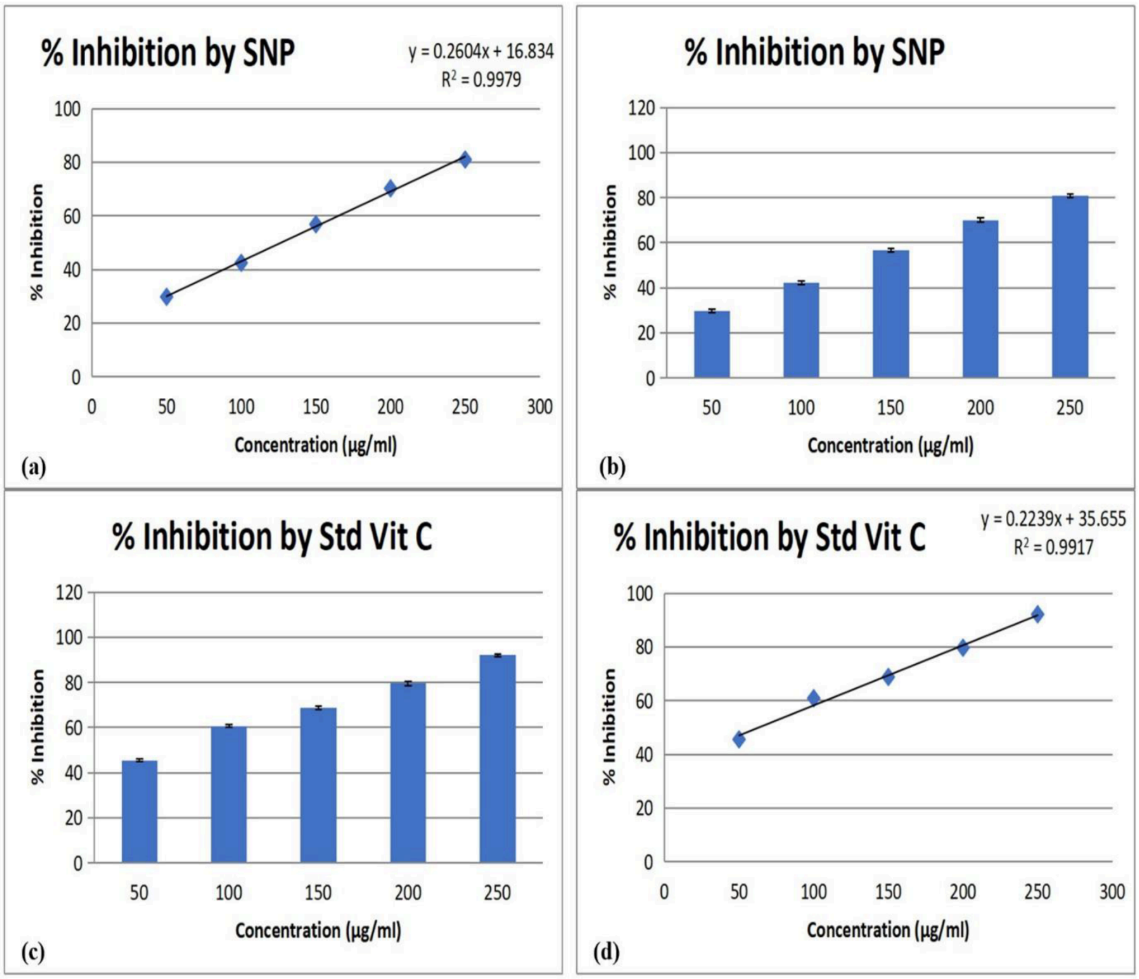


**Fig. (12).** Antioxidant activity of Biogenic Silica Nanoparticles (bSNPs) and standard vitamin C measured by the DPPH radical scavenging assay. Panels a and b show the dose-dependent percentage inhibition of DPPH radicals by bSNPs, where a represents a scatter plot with linear regression and b represents the corresponding bar graph. Panels c and d show the antioxidant activity of standard vitamin C, where c represents the bar graph, and d represents the scatter plot with linear regression. *(A higher resolution / colour version of this figure is available in the electronic copy of the article).*

concentrations (50–250 µg/mL), the absorbance gradually decreased, indicating that the nanoparticles effectively neutralized free radicals. The percentage of radical inhibition increased as the concentration went up, starting at 29.61% for 50 µg/mL and reaching 80.81% for 250 µg/mL. The $IC_{50}$ value, the concentration needed to inhibit 50% of the radicals, was calculated to be 127.36 µg/mL. This indicates that the nanoparticles have moderate antioxidant strength. For comparison, vitamin C, a well-known antioxidant, showed even higher scavenging activity, with inhibition ranging from 45.38% to 91.96% and an $IC_{50}$ of 64.06 µg/mL. A strong correlation ($R^2 \approx 0.99$) between concentration and antioxidant activity suggests the results are reliable and consistent. The antioxidant effect of the nanoparticles is likely due to the electron-donating properties of the silica surface and the residual phytochemicals from the onion peel extract, which help neutralize free radicals. These results agree with earlier studies on green-synthesized silica and metal nanoparticles showing antioxidant properties. [51, 52] All experiments were done in triplicate (n = 3), and results are reported as mean ± Standard Deviation (SD).

### 3.11. Anti-Inflammatory Activity

Anti-inflammatory properties of the Biogenic Silica Nanoparticles (bSNPs) were tested using a protein denaturation inhibition assay (Fig. **13a–d**). When the nanoparticles were added at concentrations from 50 to 250 µg/mL, they clearly blocked protein denaturation in a dose-dependent way. The percentage of inhibition rose from $13.48 \pm 0.89\%$ at 50 µg/mL to $73.71 \pm 0.73\%$ at 250 µg/mL, showing that their anti-inflammatory effect became stronger as the concentration increased. The $IC_{50}$ for bSNPs, the amount needed to inhibit 50% of protein denaturation, was 164.21 µg/mL, indicating moderate anti-inflammatory activity. For comparison, a standard drug performed better, with inhibition going from $36.81 \pm 0.96\%$ at 50 µg/mL to $86.17 \pm 0.45\%$ at 250 µg/mL, and an $IC_{50}$ of 96.34 µg/mL. The strong correlation between concentration and inhibition ($R^2 \approx 0.99$) shows

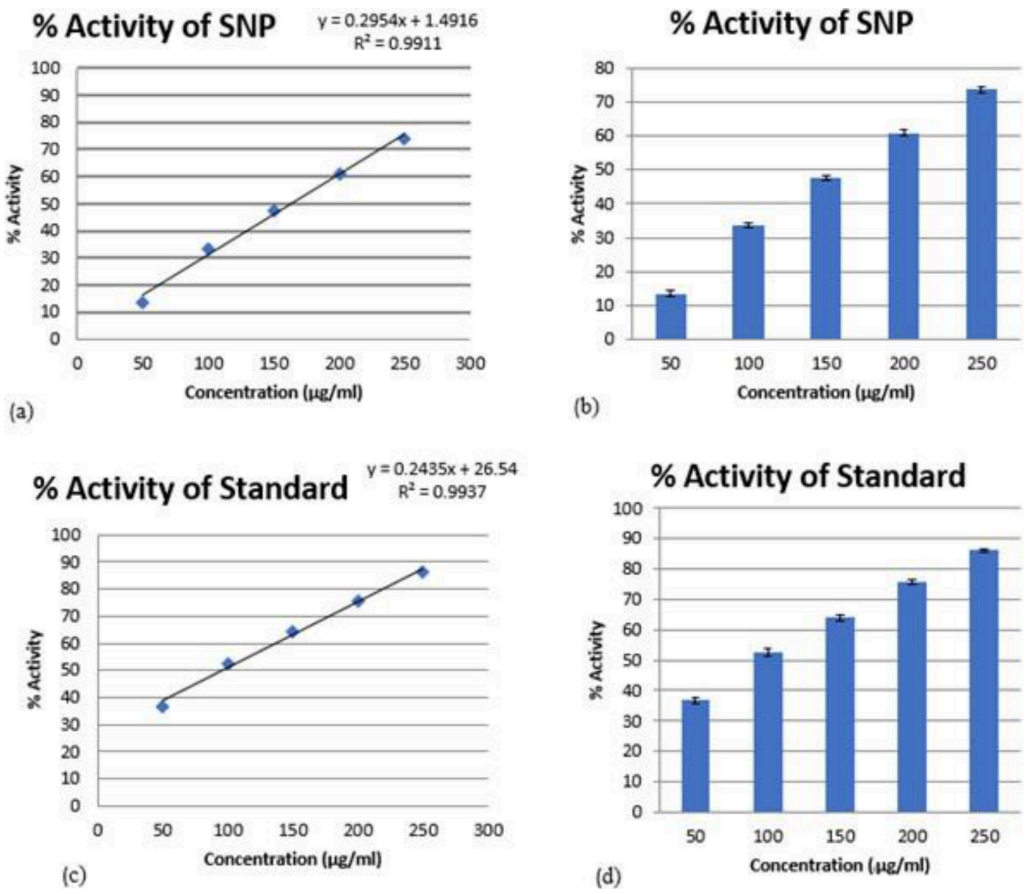


**Fig. (13).** Dose-dependent anti-inflammatory activity of Biogenic Silica Nanoparticles (bSNPs) and standard compounds measured by the protein denaturation assay. Panels a and b show the percentage inhibition of protein denaturation by bSNPs, where a represents a scatter plot with linear regression and b represents a bar graph. Panels c and d show the percentage inhibition by standard compounds, where c represents a scatter plot with a regression line, and d represents a bar graph. The x-axis represents sample concentration (µg/mL), and the y-axis represents percentage inhibition of protein denaturation. *(A higher resolution / colour version of this figure is available in the electronic copy of the article).*

that the results are reliable and consistent. The nanoparticles likely stabilize protein structures and protect them from heat-induced denaturation, a common mechanism by which anti-inflammatory agents act. Similar results have been reported for other plant-based nanoparticles. All experiments were repeated three times (n = 3), and results are shown as mean ± Standard Deviation (SD), demonstrating good precision. Overall, these findings suggest that the synthesized bSNPs have promising anti-inflammatory potential and could be explored further for biomedical applications [53, 54].

## 4 DISCUSSION

The UV–Visible absorption spectrum confirmed the successful formation of biogenic silica nanoparticles. A strong absorption band was observed in the lower UV region, attributed to electronic transitions within the Si–O–Si framework. There was no surface plasmon resonance peak in the visible range, which confirms that the silica nanoparticles are not metallic. The broad absorption pattern matches what's expected for amorphous silica, and could be due to structural defects and the presence of surface silanol (Si–OH) groups, features often seen in plant-based silica. Other studies with Agro-waste have shown similar results [55, 56]. We used FTIR analysis to confirm the formation of silica. The results showed clear peaks that matched Si–O–Si stretching and O–H bending, which are typical for amorphous silica and its surface silanol groups. Our spectrum, spanning 4000–400 $cm^{-1}$, resembled those reported for silica derived from banana peels, corn cobs, and wheat husk after acid cleaning [58, 59]. The low carbon signal also suggests that most organic residues were removed, resulting in very pure silica nanoparticles [60].

XRD analysis indicated that the synthesized biogenic silica nanoparticles were predominantly amorphous. Although several sharp reflections were observed in the diffraction pattern, these peaks did not correspond to crystalline silica phases such as quartz, cristobalite, or tridymite. Instead, they are likely attributed to trace mineral residues originating from inorganic elements present in the plant precursor. Therefore, the observed reflections represent residual impurities rather than crystallization of the silica framework, confirming that the synthesized silica matrix remains largely amorphous [61, 62]. Zeta potential tests showed that the na-

noparticles had a nearly neutral surface charge (about −0.2 mV) at pH 5, meaning they tend to clump together a bit. This might be because some silanol groups are only partly ionized, and a few leftover biomolecules are still on the surface. These factors can affect the stability of particles in solution and their interactions in biological settings [63]. Similar surface charges have been observed in silica derived from rice husk and sugarcane bagasse, where natural residues help stabilize and maintain the nanoparticles' activity [64].

When we examined the particles using SEM and AFM, we found they were mostly irregular spheres with rough, porous surfaces. This shape is similar to what is found in silica made from onion skin ash, rice husk ash, and sugarcane bagasse. The particle sizes we measured by DLS were bigger than those from TEM, which is normal: DLS accounts for the water layer and any clumping, while TEM shows the actual dry core size [65]. The porous and rough surfaces could give the particles more surface area, helping them interact better with biomolecules, useful for drug delivery and other medical uses.

Elemental analysis confirmed that the silica was highly pure, with minimal contamination. This shows that our two-step acid sol–gel process worked well. Other studies using acid leaching on agro-waste have achieved similar levels of purity, greatly reducing metal and carbon leftovers.

Agarose gel electrophoresis showed that the bSNPs we made could bind tightly to genomic DNA. As we increased the concentration of nanoparticles, more DNA became trapped in the gel wells rather than moving through the gel [66]. This means stable DNA–nanoparticle complexes formed. The binding is likely helped by positive ions bridging the negatively charged DNA and silica surfaces, as well as hydrogen bonds with DNA bases [67, 68]. Molecules left over from onion peels on the nanoparticle surface might also help the DNA bind more firmly [69]. This strong DNA-binding ability suggests these nanoparticles could be useful for delivering genetic material, biosensing, and other biomedical applications [70, 71].

The bSNPs we created also showed strong antioxidant activity in DPPH tests; the higher the concentration, the more efficiently they neutralized free radicals. This matches earlier research showing that plant-based silica nanoparticles are strong antioxidants, likely because of their surface groups and residual plant compounds that help them donate electrons [72, 73]. The nanoparticles also reduced inflammation in a protein denaturation test, again in a concentration-dependent way. This may be because silica nanoparticles can help stabilize proteins, stopping them from unfolding when heated, a known anti-inflammatory effect [74-76].

## CONCLUSION

Onion peels can be used as an eco-friendly starting material for the synthesis of silica nanoparticles via an acid-assisted sol-gel method. These nanoparticles have properties that make them promising for use in medicine, especially for potential biomedical and drug-delivery applications. This research contributes to the growing body of knowledge on the conversion of agricultural waste into valuable biomedical materials.

## LIMITATIONS AND FUTURE PERSPECTIVES

Although this work shows the successful preparation and preliminary characterization of onion peel–derived biogenic silica nanoparticles, further investigations are necessary to demonstrate their applicability for biomedical applications. Formulating nanoparticles into topical gel formulations and testing various formulation combinations were not within the scope of the current work. Moreover, the evaluation of the cytotoxicity assay, as well as extensive biological validation through *in vivo* skin irritation tests, would be out of the scope of this work. These tests are necessary to verifythe biocompatibility and safety of this system. Further research, including gel formulation, optimization of nanoparticle–gel combinations, a complete *in vitro* cytotoxicity profile, and skin irritation studies in rats, could justify the applicability of biogenic silica nanoparticles for topical drug delivery systems.

## AUTHORS' CONTRIBUTIONS (CREDIT TAXONOMY)

The authors confirm their contributions to the paper as follows:Conceptualization: G.K., R.D.; Methodology: S.H., R.D.; Investigation: S.H.; Data curation: A.K.S., R.D.; Formal analysis: A.K.S., R.D.; Writing – original draft: S.H.; Writing – review and editing: R.D., G.K., A.K.S.; Supervision: R.D., G.K., A.K.S. All authors have read and approved the final manuscript.

## LIST OF ABBREVIATIONS

| | | |
|---|---|---|
| AFM | = | Atomic Force Microscopy |
| bSNPs | = | Biogenic Silica Nanoparticles |
| BSA | = | Bovine Serum Albumin |
| DLS | = | Dynamic Light Scattering |
| DPPH | = | 2,2-Diphenyl-1-picrylhydrazyl |
| EDX | = | Energy-Dispersive X-ray Spectroscopy |
| FTIR | = | Fourier Transform Infrared Spectroscopy |
| $IC_{50}$ | = | Half-Maximal Inhibitory Concentration |
| NSAID | = | Nonsteroidal Anti-Inflammatory Drug |
| PBS | = | Phosphate-Buffered Saline |
| SEM | = | Scanning Electron Microscopy |
| TEM | = | Transmission Electron Microscopy |
| UV–Vis | = | Ultraviolet–Visible Spectroscopy |
| XRD | = | X-ray Diffraction |

## ETHICS APPROVAL AND CONSENT TO PARTICIPATE

Not applicable.

## HUMAN AND ANIMAL RIGHTS

This study did not involve human participants or experimental animals.

## CONSENT FOR PUBLICATION

Not applicable.

## AVAILABILITY OF DATA AND MATERIAL

The data supporting the findings of this study are available from the corresponding author upon reasonable request.

## FUNDING

None.

## CONFLICT OF INTERESTS

The authors state that they have no known conflicting financial interests or personal ties that might have influenced the work presented in this study.

## ACKNOWLEDGEMENT

Declared none.

## REFERENCES

[1] Ball AS, Patil S, Soni S, Issaabadi Z. Introduction into nanotechnology and microbiology. Methods Microbiol 2019; 46: 1-18. http://dx.doi.org/10.1016/bs.mim.2019.04.003 PMID: 38620196

[2] Ardestani EA, Zakariaee SJS, Fard MHS, Mirshekari B. Synthesis of biogenic mesoporous silica nanoparticles from rice husks waste materials *via* sol–gel method. Biomass Convers Biorefin 2025; 15(22): 29191-206. http://dx.doi.org/10.1007/s13399-025-06840-x

[3] Alam F, Nag M, Judder MI, *et al.* Eco-compatible synthesis of metal nanoparticles: Influencing parameters, characterization, advancement and applications. Asian J Chem 2025; 37(11): 2617-30. http://dx.doi.org/10.14233/ajchem.2025.34459

[4] Raghunandan D, Borgaonkar PA, Bendegumble B, *et al.* Microwave-assisted rapid extracellular biosynthesis of silver nanoparticles using carom seed (Trachyspermum copticum) extract and *in vitro* studies. Am J Anal Chem 2011; 2(4): 475-83. http://dx.doi.org/10.4236/ajac.2011.24057

[5] Gupta J. Nanotechnology applications in medicine and dentistry. J Investig Clin Dent 2011; 2(2): 81-8. http://dx.doi.org/10.1111/j.2041-1626.2011.00046.x PMID: 25426600

[6] Deshpande R, Bedre MD, Salimath B, Sawle BD, Yalagatti MS, Abbaraju V. Microwave-assisted rapid biosynthesis of stable silver nanoparticles using clove buds (Syzygium aromaticum) solution. Nano Life 2012; 2(2): 1250012. http://dx.doi.org/10.1142/S1793984411000499

[7] Patra JK, Das G, Fraceto LF, *et al.* Nano based drug delivery systems: Recent developments and future prospects. J Nanobiotechnology 2018; 16(1): 71. http://dx.doi.org/10.1186/s12951-018-0392-8 PMID: 30231877

[8] Iranshahy M, Hanafi-Bojd MY, Aghili SH, *et al.* Curcumin-loaded mesoporous silica nanoparticles for drug delivery: Synthesis, biological assays and therapeutic potential – A review. RSC Advances 2023; 13(32): 22250-67. http://dx.doi.org/10.1039/D3RA02772D PMID: 37492509

[9] Gressler S, Hipfinger C, Part F, Pavlicek A, Zafiu C, Giese B. A systematic review of nanocarriers used in medicine and beyond — Definition and categorization framework. J Nanobiotechnology 2025; 23(1): 90. http://dx.doi.org/10.1186/s12951-025-03113-7 PMID: 39920688

[10] Yadav M, Dwibedi V, Sharma S, George N. Biogenic silica nanoparticles from agro-waste: Properties, mechanism of extraction and applications in environmental sustainability. J Environ Chem Eng 2022; 10(6): 108550. http://dx.doi.org/10.1016/j.jece.2022.108550

[11] Goswami P, Mathur J. Application of agro-waste-mediated silica nanoparticles to sustainable agriculture. Bioresour Bioprocess 2022; 9(1): 9. http://dx.doi.org/10.1186/s40643-022-00496-5 PMID: 38647762

[12] Porrang S, Rahemi N, Davaran S, Mahdavi M, Hassanzadeh B. Preparation and in-vitro evaluation of mesoporous biogenic silica nanoparticles obtained from rice and wheat husk as a biocompatible carrier for anti-cancer drug delivery. Eur J Pharm Sci 2021; 163: 105866. http://dx.doi.org/10.1016/j.ejps.2021.105866 PMID: 33957220

[13] Sankar S, Sharma SK, Kaur N, *et al.* Biogenerated silica nanoparticles synthesized from sticky, red, and brown rice husk ashes by a chemical method. Ceram Int 2016; 42(4): 4875-85. http://dx.doi.org/10.1016/j.ceramint.2015.11.172

[14] Nath PC, Ojha A, Debnath S, *et al.* Biogeneration of valuable nanomaterials from agro-wastes: A comprehensive review. Agronomy 2023; 13(2): 561. http://dx.doi.org/10.3390/agronomy13020561

[15] Iravani S. Green synthesis of metal nanoparticles using plants. Green Chem 2011; 13(10): 2638-50. http://dx.doi.org/10.1039/c1gc15386b

[16] Raghunandan D, Mahesh BD, Basavaraja S, Balaji SD, Manjunath SY, Venkataraman A. Microwave-assisted rapid extracellular synthesis of stable bio-functionalized silver nanoparticles from guava (Psidium guajava) leaf extract. J Nanopart Res 2011; 13(5): 2021-8. http://dx.doi.org/10.1007/s11051-010-9956-8

[17] Chaudhary S, Jain VP, Sharma D, Jaiswar G. Implementation of agriculture waste for the synthesis of metal oxide nanoparticles: Its management, future opportunities and challenges. J Mater Cycles Waste Manag 2023; 25(6): 3144-60. http://dx.doi.org/10.1007/s10163-023-01770-0

[18] Danhier F, Ansorena E, Silva JM, Coco R, Le Breton A, Préat V. PLGA-based nanoparticles: An overview of biomedical applications. J Control Release 2012; 161(2): 505-22. http://dx.doi.org/10.1016/j.jconrel.2012.01.043 PMID: 22353619

[19] Rahman IA, Padavettan V. Synthesis of silica nanoparticles by sol-gel: Size-dependent properties, surface modification, and applications in silica-polymer nanocomposites—A review. J Nanomater 2012; 2012(1): 132424. http://dx.doi.org/10.1155/2012/132424

[20] Vaibhav V, Vijayalakshmi U, Roopan SM. Agricultural waste as a source for the production of silica nanoparticles. Spectrochim Acta A Mol Biomol Spectrosc 2015; 139: 515-20. http://dx.doi.org/10.1016/j.saa.2014.12.083 PMID: 25576950

[21] Trzeciak K, Chotera-Ouda A, Bak-Sypien II, Potrzebowski MJ. Mesoporous silica particles as drug delivery systems—the state of the art in loading methods and the recent progress in analytical techniques for monitoring these processes. Pharmaceutics 2021; 13(7): 950. http://dx.doi.org/10.3390/pharmaceutics13070950 PMID: 34202794

[22] Mattos BD, Rojas OJ, Magalhães WLE. Biogenic silica nanoparticles loaded with neem bark extract as green, slow-release biocide. J Clean Prod 2017; 142: 4206-13. http://dx.doi.org/10.1016/j.jclepro.2016.11.183

[23] Gaballa H, shalaby , fayed , shanab . Chemical constituents and biological activity of successive extracts and silver nanoparticles from red onion peels. Egypt J Chem 2022; 0(0): 0. http://dx.doi.org/10.21608/ejchem.2022.136419.6010

[24] Alshahrani AA, Alqarni LS, Alghamdi MD, Alotaibi NF, Moustafa SMN, Nassar AM. Phytosynthesis *via* wasted onion peel extract of samarium oxide/silver core/shell nanoparticles for excellent inhibition of microbes. Heliyon 2024; 10(3): 24815. http://dx.doi.org/10.1016/j.heliyon.2024.e24815 PMID: 38322933

[25] Celano R, Docimo T, Piccinelli AL, *et al.* Onion peel: Turning a food waste into a resource. Antioxidants 2021; 10(2): 304. http://dx.doi.org/10.3390/antiox10020304 PMID: 33669451

[26] Espina Palanco M, Bo Mogensen K, Gühlke M, Heiner Z, Kneipp J, Kneipp K. Templated green synthesis of plasmonic silver nanoparticles in onion epidermal cells suitable for surface-enhanced

Raman and hyper-Raman scattering. Beilstein J Nanotechnol 2016; 7: 834-40.
http://dx.doi.org/10.3762/bjnano.7.75 PMID: 27547600

[27] Sonawane LD, Mandawade AS, Gite AB, *et al.* Sol–gel synthesis of silicon oxide ($SiO_2$) nanoparticles: Exploring gas sensing and photocatalytic applications. Journal of Materials Science: Materials in Engineering 2025; 20(1): 8.
http://dx.doi.org/10.1186/s40712-025-00209-8

[28] Le VH, Thuc CNH, Thuc HH. Synthesis of silica nanoparticles from Vietnamese rice husk by sol–gel method. Nanoscale Res Lett 2013; 8(1): 58.
http://dx.doi.org/10.1186/1556-276X-8-58 PMID: 23388152

[29] Gonçalves MC. Sol–gel silica nanoparticles in medicine: A natural choice—Design, synthesis and products. Molecules 2018; 23(8): 2021.
http://dx.doi.org/10.3390/molecules23082021 PMID: 30104542

[30] Ni'mah YL, Muhaiminah ZH, Suprapto . Suprapto. Synthesis of silica nanoparticles from sugarcane bagasse by sol–gel method. AIP Conf Proc 2023; 2596: 050011.
http://dx.doi.org/10.1063/5.0107310

[31] Modi S, Yadav VK, Choudhary N, *et al.* Onion peel waste mediated green synthesis of zinc oxide nanoparticles and their phytotoxicity on mung bean and wheat plant growth. Materials 2022; 15(7): 2393.
http://dx.doi.org/10.3390/ma15072393 PMID: 35407725

[32] Venezia V, Coccia E, Marra S, *et al.* Antioxidant potential and biocompatibility of pomegranate peel extract functionalized silica nanoparticles. J Sol-Gel Sci Technol 2025; 116(3): 1951-67.
http://dx.doi.org/10.1007/s10971-025-06884-5

[33] Tan Sian Hui Abdullah HS, Aqlili Riana Mohd Asseri SN, Khursyiah Wan Mohamad WN, *et al.* Green synthesis, characterization and applications of silver nanoparticle mediated by the aqueous extract of red onion peel. Environ Pollut 2021; 271: 116295.
http://dx.doi.org/10.1016/j.envpol.2020.116295 PMID: 33383429

[34] Shrestha D, Nayaju T, Kandel MR, Pradhananga RR, Park CH, Kim CS. Rice husk-derived mesoporous biogenic silica nanoparticles for gravity chromatography. Heliyon 2023; 9(4): 15142.
http://dx.doi.org/10.1016/j.heliyon.2023.e15142 PMID: 37095947

[35] Abdel Hamid E, Ismail M, Moussa M, *et al.* Optimization and characterization of bio-silica extraction from rice straw using RSM. Egypt J Chem 2023; 0(0): 0.
http://dx.doi.org/10.21608/ejchem.2023.161205.6968

[36] September LA, Kheswa N, Seroka NS, Khotseng L. Green synthesis of silica and silicon from agricultural residue sugarcane bagasse ash – A mini review. RSC Advances 2023; 13(2): 1370-80.
http://dx.doi.org/10.1039/D2RA07490G PMID: 36686953

[37] Izquierdo-Barba I, Manzano M, Colilla M, Vallet-Regí M. Silica-based ordered mesoporous materials for biomedical applications. Key Eng Mater 2008; 377: 133-50.
http://dx.doi.org/10.4028/www.scientific.net/KEM.377.133

[38] Brand-Williams W, Cuvelier ME, Berset C. Use of a free radical method to evaluate antioxidant activity. Lebensm Wiss Technol 1995; 28(1): 25-30.
http://dx.doi.org/10.1016/S0023-6438(95)80008-5

[39] Nikolaidis A, Moschakis T. Studying the denaturation of bovine serum albumin by a novel approach of difference-UV analysis. Food Chem 2017; 215: 235-44.
http://dx.doi.org/10.1016/j.foodchem.2016.07.133 PMID: 27542472

[40] Rathod K, Ahmed H, Gomte SS, *et al.* Exploring the potential of anti-inflammatory activity of berberine chloride-loaded mesoporous silica nanoparticles in carrageenan-induced rat paw edema model. J Solid State Chem 2023; 317: 123639.
http://dx.doi.org/10.1016/j.jssc.2022.123639

[41] Patel M, Chhasatia M, Parmar P. Antibacterial and DNA interaction studies of zinc(II) complexes with quinolone family member, ciprofloxacin. Eur J Med Chem 2010; 45(2): 439-46.
http://dx.doi.org/10.1016/j.ejmech.2009.10.024 PMID: 19913957

[42] Abomughaid MM. Bio-fabrication of bio-inspired silica nanomaterials from orange peels in combating oxidative stress. Nanomaterials 2022; 12(18): 3236.
http://dx.doi.org/10.3390/nano12183236 PMID: 36145024

[43] Maroušek J, Marouškova A, Periakaruppan R, *et al.* Silica nanoparticles from coir pith synthesized by acidic sol-gel method improve germination economics. Polymers 2022; 14(2): 266.
http://dx.doi.org/10.3390/polym14020266 PMID: 35054673

[44] Saha A, Mishra P, Biswas G, Bhakta S. Greening the pathways: A comprehensive review of sustainable synthesis strategies for silica nanoparticles and their diverse applications. RSC Advances 2024; 14(16): 11197-216.
http://dx.doi.org/10.1039/D4RA01047G PMID: 38590352

[45] Kumar SP, Yassin MM, Marimuthu S, Kalarani MK, Thiyageshwari S, Meenakshi G. Eco-friendly synthesis and characterization of amorphous nanosilica from rice husk. Agric Sci Dig 2023; 43(Of): D-5792.
http://dx.doi.org/10.18805/ag.D-5792

[46] Vallet-Regí M, Balas F, Arcos D. Mesoporous materials for drug delivery. Angew Chem Int Ed 2007; 46(40): 7548-58.
http://dx.doi.org/10.1002/anie.200604488 PMID: 17854012

[47] Gandhi N, Reddy YRG, Vijaya C, Aruna K. Biogenic silica nanoparticles from Arachis hypogaea shell waste: Synthesis, characterization and agricultural applications. Int J Sci Res Chem Sci 2025; 12(1): 11-27.
http://dx.doi.org/10.26438/ijsrcs.v12i1.183

[48] Peerzada JG, Chidambaram R. A statistical approach for biogenic synthesis of nano-silica from different agro-wastes. Silicon 2021; 13(7): 2089-101.
http://dx.doi.org/10.1007/s12633-020-00629-5

[49] Abd El-Zahir MS, Saleh SM, ElKady HA, Orabi AS. Ciprofloxacin metal complexes–silica nanoparticles: Characterization, spectroscopic study, DNA interaction and biological activity. J Solution Chem 2024; 53(9): 1269-93.
http://dx.doi.org/10.1007/s10953-024-01375-7

[50] Slowing I, Viveroescoto J, Wu C, Lin V. Mesoporous silica nanoparticles as controlled release drug delivery and gene transfection carriers. Adv Drug Deliv Rev 2008; 60(11): 1278-88.
http://dx.doi.org/10.1016/j.addr.2008.03.012 PMID: 18514969

[51] Baliyan S, Mukherjee R, Priyadarshini A, *et al.* Determination of antioxidants by DPPH radical scavenging activity and quantitative phytochemical analysis of Ficus religiosa. Molecules 2022; 27(4): 1326.
http://dx.doi.org/10.3390/molecules27041326 PMID: 35209118

[52] Ali A, Ali SR, Hussain R, *et al.* Comparative study of silica and silica-decorated ZnO and ag nanocomposites for antimicrobial and photocatalytic applications. Sci Rep 2025; 15(1): 5010.
http://dx.doi.org/10.1038/s41598-025-89812-5 PMID: 39930080

[53] Brezoiu AM, Deaconu M, Mitran RA, *et al.* The antioxidant and anti-inflammatory properties of wild bilberry fruit extracts embedded in mesoporous silica-type supports: A stability study. Antioxidants 2024; 13(2): 250.
http://dx.doi.org/10.3390/antiox13020250 PMID: 38397847

[54] Khan H, Khan MA, Rauf A, Haleemi A, Fuloria S, Fuloria NK. Inhibition of urease and thermal-induced protein denaturation of commonly used antiulcer herbal products: Study based on *in vitro* assays. Pharmacogn J 2015; 7(3): 147-51.
http://dx.doi.org/10.5530/pj.2015.3.1

[55] Jeelani PG, Ramalingam C. Statistical approach to synthesise biogenic silica nanoparticles from rice husk and conjugated with *Justicia adhatoda* extract as green, slow-release biocide. IET Nanobiotechnol 2021; 15(4): 391-401.
http://dx.doi.org/10.1049/nbt2.12027 PMID: 34694712

[56] Bogush GH, Tracy MA, Zukoski CF. Preparation of monodisperse silica particles: Control of size and mass fraction. J Non-Cryst Solids 1988; 104(1): 95-106.
http://dx.doi.org/10.1016/0022-3093(88)90187-1

[57] Habte GA, Bullo TA, Ahmed Y. Statistical optimization characterizations and Eco- friendly synthesis of silica from sugarcane bagasse. Sci Rep 2025; 15(1): 8492.
http://dx.doi.org/10.1038/s41598-025-89366-6 PMID: 40074734

[58] Elizondo-Villarreal N, Gandara-Martínez E, García-Méndez M, *et al.* Synthesis and characterization of $SiO_2$ nanoparticles for application as nanoadsorbent to clean wastewater. Coatings 2024; 14(7): 919.
http://dx.doi.org/10.3390/coatings14070919

[59] Mohammed AM, Ahmed AM, Said AH, Mohammed HF. Eco-friendly synthesis and antibacterial properties of silica nanoparticles from Rhus coriaria extract. Sohag J Sci 2025; 10: 291-5.

http://dx.doi.org/10.21608/sjsci.2025.360087.1258

[60] Singh G, Dizaji HB, Puttuswamy H, Sharma S. Biogenic nanosilica synthesis employing agro-waste rice straw and its application in photocatalytic degradation of cationic dye. Sustainability 2022; 14(1): 539. http://dx.doi.org/10.3390/su14010539

[61] Manikandan R, Thomas J. Sustainable approaches in green synthesis of silica nanoparticles using extracts of Chlorella and its application. Appl Biochem Biotechnol 2024; 196(11): 7928-39. http://dx.doi.org/10.1007/s12010-024-04949-9 PMID: 38662321

[62] Croissant JG, Fatieiev Y, Almalik A, Khashab NM. Mesoporous silica and organosilica nanoparticles: Physical chemistry, biosafety, delivery strategies, and biomedical applications. Adv Healthc Mater 2018; 7(4): 1700831. http://dx.doi.org/10.1002/adhm.201700831 PMID: 29193848

[63] Kosmulski M. Compilation of PZC and IEP of sparingly soluble metal oxides and hydroxides from literature. Adv Colloid Interface Sci 2009; 152(1-2): 14-25. http://dx.doi.org/10.1016/j.cis.2009.08.003 PMID: 19744641

[64] Lu P, Hsieh YL. Highly pure amorphous silica nano-disks from rice straw. Powder Technol 2012; 225: 149-55. http://dx.doi.org/10.1016/j.powtec.2012.04.002

[65] Kalapathy U. A simple method for production of pure silica from rice hull ash. Bioresour Technol 2000; 73(3): 257-62. http://dx.doi.org/10.1016/S0960-8524(99)00127-3

[66] Lee PY, Costumbrado J, Hsu CY, Kim YH. Agarose gel electrophoresis for the separation of DNA fragments. J Vis Exp 2012; 3923(62): •••. http://dx.doi.org/10.3791/3923 PMID: 22546956

[67] Bag S, Rauwolf S, Schwaminger SP, Wenzel W, Berensmeier S. DNA binding to silica: Cooperative adsorption in action. Langmuir 2021; 37(19): 5902-8. http://dx.doi.org/10.1021/acs.langmuir.1c00381 PMID: 33951395

[68] Li K, Zhao X, K Hammer B, Du S, Chen Y. Nanoparticles inhibit DNA replication by binding to DNA: Modeling and experimental validation. ACS Nano 2013; 7(11): 9664-74. http://dx.doi.org/10.1021/nn402472k PMID: 24093667

[69] Shi B, Shin YK, Hassanali AA, Singer SJ. DNA binding to the silica surface. J Phys Chem B 2015; 119(34): 11030-40. http://dx.doi.org/10.1021/acs.jpcb.5b01983 PMID: 25966319

[70] Tietz D, Aldroubi A, Pulyaeva H, Guszczynski T, Garner MM, Chrambach A. Advances in DNA electrophoresis in polymer solutions. Electrophoresis 1992; 13(1): 614-6. http://dx.doi.org/10.1002/elps.11501301124 PMID: 1459075

[71] Vahdati AR, Sadeghi B. A study on the assessment of DNA strand-breaking activity by silver and silica nanoparticles. J Nanostructure Chem 2013; 3(1): 7. http://dx.doi.org/10.1186/2193-8865-3-7

[72] Periakaruppan R, Chandrasekaran N, T SK, Sasthri G, Al-Dayan N. Green synthesis of silica nanoparticles using Enhalus acoroides: Characterization and antioxidant activity. Biomass Convers Biorefin 2025; 15(22): 28585-92. http://dx.doi.org/10.1007/s13399-024-06450-z

[73] Palanimuthu V, Rajendran N, Periakaruppan R, Romanovski V, Govindaraju P, Natarajan M. Green synthesis and characterization of SiO2 nanoparticles using tridax procumbens leaf extract and enhancing the invitro wound healing activity in l929 fibroblast cell lines. Waste & Biomass Valoriz 2025. http://dx.doi.org/10.1007/s12649-025-03364-3

[74] Wu Y, Chen W, Zeng Y, *et al.* Inflammation-responsive mesoporous silica nanoparticles with synergistic anti-inflammatory and joint protection effects for rheumatoid arthritis treatment. Pharm Res 2024; 41(7): 1493-505. http://dx.doi.org/10.1007/s11095-024-03732-z PMID: 38918308

[75] Abdelkader HS, Kheder AA, Amin HA, Shafie RM. A comparative study of the antiviral effects of biogenic silver nanoparticles and nanosilica (nSiO2) against Leek yellow stripe virus on *Allium sativum* L. Eur J Plant Pathol 2025; 171(3): 509-30. http://dx.doi.org/10.1007/s10658-024-02965-3

[76] Grunberger JW, Dobrovolskaia MA, Ghandehari H. Immunological properties of silica nanoparticles: A structure–activity relationship study. Nanotoxicology 2024; 18(6): 542-64. http://dx.doi.org/10.1080/17435390.2024.2401448 PMID: 39282894